

Blue photoluminescence in Ti-doped alkaline-earth stannates

Takahiro Yamashita, Kazushige Ueda*

Department of Materials Science, Faculty of Engineering, Kyushu Institute of Technology, 1-1 Sensui, Tobata, Kitakyushu, Fukuoka 804-8550, Japan

Received 13 December 2006; received in revised form 11 February 2007; accepted 12 February 2007

Available online 21 February 2007

Abstract

Blue photoluminescence properties of Ti-doped alkaline-earth stannates, $A_2(\text{Sn}_{1-x}\text{Ti}_x)\text{O}_4$ ($A = \text{Ca}, \text{Sr}, \text{Ba}$) ($x = 0.005\text{--}0.15$), were examined at room temperature. These stannates showed intense broad emission bands peaking at 445 nm for Ca_2SnO_4 , at 410 nm for Sr_2SnO_4 , and at 425 nm for Ba_2SnO_4 under UV excitation. Emission intensities were relatively insensitive to Ti concentration and no sharp concentration quenching was observed. Mixing alkaline-earth ions in the crystal structures did not increase the emission intensities in the $A_2(\text{Sn}_{1-x}\text{Ti}_x)\text{O}_4$ system. The excitation spectra of these stannates exhibited broad bands just below the fundamental absorption edges, implying that luminescence centers do not consist of the component elements in the host materials. It was suggested that the isolated TiO_6 complexes are possible luminescence centers in these materials, as previously proposed in other Ti-doped stannates such as Mg_2SnO_4 and $\text{Y}_2\text{Sn}_2\text{O}_7$.

© 2007 Elsevier Inc. All rights reserved.

PACS: 78.55.Hx; 81.05.Je

Keywords: Luminescence; Optical materials; Oxides; Layered compounds; Ceramics photoluminescence; Blue phosphor; Stannates; Perovskite-related structure

1. Introduction

Phosphor materials have been widely used in various display and luminescence applications and actively investigated to improve their luminescence properties such as emission color and efficiency [1]. Flat-panel displays such as plasma display panels (PDP), field emission displays (FED), and electroluminescent (EL) devices are particularly important applications of phosphor materials. Therefore, the development of new inorganic phosphors with high chemical stability and luminescence efficiency is essential to improve the performance of the flat-panel displays. In the viewpoint of chemical stability, oxide phosphors are more attractive than sulfide or oxysulfide phosphors.

There are many oxide phosphors showing various luminescence colors [1–3]. As for blue phosphors, $\text{BaMgAl}_{10}\text{O}_{17}:\text{Eu}^{2+}$ for lamps, $\text{ZnS}:\text{Ag}$ for cathode-ray tubes, and $\text{BaAl}_2\text{Si}_4:\text{Eu}^{2+}$ for EL are in practical use. In

alkaline-earth containing double oxides, $\text{Sr}_2\text{SnO}_4:\text{Eu}^{2+}$, $\text{SrHfO}_3:\text{Tm}^{3+}$, $\text{Mg}_2\text{SnO}_4:\text{Ti}^{4+}$, and Sr_2CeO_4 have been reported as blue phosphors [4–7]. In these blue phosphors, Eu^{2+} , Tm^{3+} , and Ti^{4+} ions are doped into host oxides as emission centers, giving sharp or broad peaks in the blue region under high voltage or UV/electron irradiation. Only for Eu^{2+} -doped oxide phosphors, reduction processes are usually needed in their synthesis to avoid the generation of Eu^{3+} by oxidation.

Intense photoluminescence (PL) of several colors, including blue color, was observed from doped alkaline-earth stannates in our previous study [8]. In this paper, we investigated the properties of blue luminescence in Ti-doped alkaline-earth stannates with the chemical composition of $A_2(\text{Sn}_{1-x}\text{Ti}_x)\text{O}_4$ ($A = \text{Ca}, \text{Sr}, \text{Ba}$). Although the blue luminescence of these stannate phosphors are shortly described in literature [6,9], the details of the luminescent properties have not been reported yet. Therefore, we measured their basic PL properties and further investigated the influence of A ions ($A = \text{Ca}, \text{Sr}, \text{Ba}$) on the blue luminescence to examine the chemical composition that provides maximum PL intensity.

*Corresponding author. Fax: +81 93 884 3300.

E-mail address: kueda@che.kyutech.ac.jp (K. Ueda).

2. Experiments

Samples with chemical compositions of $A_2(\text{Sn}_{1-x}\text{Ti}_x)\text{O}_4$ ($A = \text{Ca}, \text{Sr}, \text{Ba}$) ($x = 0.005\text{--}0.15$) were prepared by the solid-state reaction method using starting materials of ACO_3 ($A = \text{Ca}, \text{Sr}, \text{Ba}$) (99.9%) and SnO_2 (99.9%) for host oxides and TiO_2 (99.9%) for dopants. Appropriate amounts of these starting materials were thoroughly mixed in a mortar with ethanol and dried. The dried powders were pressed into disks and the disks were heated at 1000–1400 °C for 6 h in air. The heat treatments above 1300 °C were preferable to obtain sufficient emission intensities in these phosphors.

X-ray diffraction (XRD) patterns were measured using a Rint 2500 diffractometer (Rigaku) with $\text{CuK}\alpha$ radiation. Main diffraction peaks in the XRD patterns of the samples were identified with those from host lattices although impurity phases were slightly observed in the samples with high Ti concentration. PL emission/excitation spectra were measured using an F-4500 spectrometer (Hitachi) at room temperature. Diffuse reflection spectra were also measured at room temperature using a V-570 spectrometer (Jasco) with an integrating sphere. The diffuse reflectance spectra were converted to absorption spectra following the Kubelka–Munk theory.

3. Results and discussion

Fig. 1 shows the crystal structures of $A_2\text{SnO}_4$ ($A = \text{Ca}, \text{Sr}, \text{Ba}$) host oxides. Ca_2SnO_4 belongs to the Sr_2PbO_4 -type structure, while Sr_2SnO_4 and Ba_2SnO_4 belong to the K_2NiF_4 -type structure with/without slight distortion [10–12]. In both structural types, SnO_6 octahedra are connected in low-dimensional form; SnO_6 octahedra are linked sharing edges with each other and forming one-

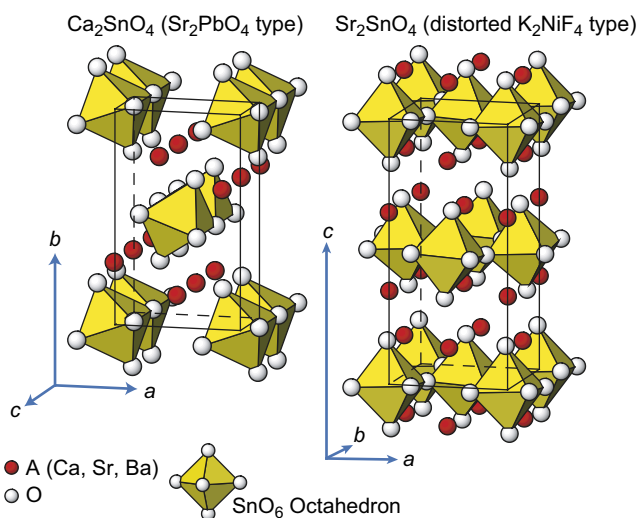


Fig. 1. Crystal structures of $A_2\text{SnO}_4$ ($A = \text{Ca}, \text{Sr}, \text{Ba}$). SnO_6 octahedra connect each other forming one-dimensional chains in Ca_2SnO_4 and two-dimensional sheets in Sr_2SnO_4 and Ba_2SnO_4 .

dimensional chains in Ca_2SnO_4 , on the other hand, they are connected sharing corners and composing two-dimensional sheets in Sr_2SnO_4 and Ba_2SnO_4 . The fundamental structural data are summarized in Table 1.

XRD patterns of $A_2(\text{Sn}_{1-x}\text{Ti}_x)\text{O}_4$ ($A = \text{Ca}, \text{Sr}, \text{Sr}_{0.5}\text{Ba}_{0.5}, \text{Ba}$) ($x = 0.05$) samples are shown in Fig. 2. The XRD pattern for the Ca_2SnO_4 sample is definitely different from those for the other samples due to the different crystal structure. On the other hand, $A_2\text{SnO}_4$ ($A = \text{Sr}, \text{Sr}_{0.5}\text{Ba}_{0.5}, \text{Ba}$) samples show similar XRD patterns with slight peak shift because the crystal structural type of K_2NiF_4 remains in the Sr_2SnO_4 – Ba_2SnO_4 system. Although the space group for Sr_2SnO_4 is different from that for Ba_2SnO_4 as listed in Table 1, the deviation of

Table 1
Crystal structural data for $A_2\text{SnO}_4$ ($A = \text{Ca}, \text{Sr}, \text{Ba}$)

	Ca_2SnO_4 [10]	Sr_2SnO_4 [11]	Ba_2SnO_4 [12]
Space group	<i>Pbam</i> (55)	<i>Bmab</i> (64)	<i>I4/mmm</i> (139)
a (Å)	5.748	5.7224	4.1411 (5.8564) ^a
b (Å)	9.694	5.7306	—
c (Å)	3.264	12.5828	13.2834
Sn–O length (Å)	2.146 × 4	2.030 × 4	2.071 × 4
	2.010 × 2	2.052 × 2	2.065 × 2
∠ O–Sn–O (deg.) ^b	81.00	89.59	90.00

^aThe lattice constant in parenthesis for Ba_2SnO_4 is a value of $\sqrt{2}a$, which is compared with the lattice constant of a or b for Sr_2SnO_4 illustrated in Fig. 1.

^bOnly the smallest O–Sn–O angle is listed in the table.

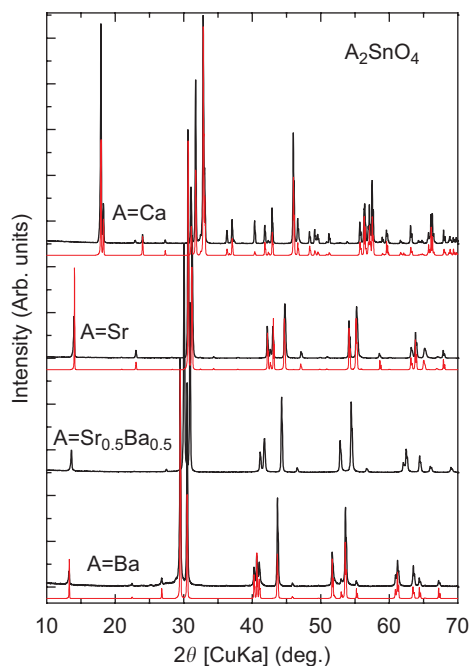


Fig. 2. Experimental XRD patterns of Ti (5%) doped $A_2\text{SnO}_4$ ($A = \text{Ca}, \text{Sr}, \text{Sr}_{0.5}\text{Ba}_{0.5}, \text{Ba}$) (thick lines) and calculated XRD patterns from the crystal structural data for $A_2\text{SnO}_4$ ($A = \text{Ca}, \text{Sr}, \text{Ba}$) (thin lines).

lattice constants in Sr_2SnO_4 from the ideal tetragonal K_2NiF_4 structure is rather small.

Emission spectra of $A_2(\text{Sn}_{1-x}\text{Ti}_x)\text{O}_4$ ($A = \text{Ca}, \text{Sr}, \text{Ba}$) ($x = 0.05$) excited by the UV radiation of $\lambda_{\text{ex}} = 254 \text{ nm}$ are shown in Fig. 3. Broad emission bands in the blue range were observed in all samples. The wavelengths at the maximum of the broad emission bands were 445 nm (2.79 eV) for the Ca stannate, 410 nm (3.02 eV) for the Sr stannate, and 425 nm (2.92 eV) for the Ba stannate. Although the mechanism of the photoluminescence in these stannates is not clearly understood, TiO_6 complexes are probably emission centers as proposed by Macke and Kröger in several Ti-activated stannates and zirconates [6,9]. Emission centers in phosphors are usually sensitive to their local structure and local symmetry. Since the Sn–O lengths and O–Sn–O angles depend on the alkaline-earth ions in $A_2\text{SnO}_4$ ($A = \text{Ca}, \text{Sr}, \text{Ba}$) (Table 1), the wavelength at the maximum emission intensity seems to vary along with the change of the alkaline-earth ions in these stannates.

Fig. 4 shows excitation spectra of $A_2(\text{Sn}_{1-x}\text{Ti}_x)\text{O}_4$ ($A = \text{Ca}, \text{Sr}, \text{Ba}$) ($x = 0.05$) along with the absorption spectra of nondoped host materials. The excitation spectrum for each sample was measured by fixing the emission wavelength at the maximum in Fig. 3. In the absorption spectra, intense absorption by host materials appears in the wavelength range shorter than approximately 270 nm for all stannates. This absorption is attributed to the fundamental absorption of the host materials. The slight differences of the absorption edges are due to the different crystal structures and ionic sizes of the alkaline-earth ions. The excitation spectra of all Ti-doped samples show common broad bands just below the absorption edges of the host crystals. This observation suggests that electrons in the valence band or oxygen ions are excited not to the conduction band but to Ti-related defect levels, and then the Ti-related centers emit the blue luminescence along with the Stokes shift. The Stokes shift of each sample was estimated to be approximately 1.6 eV

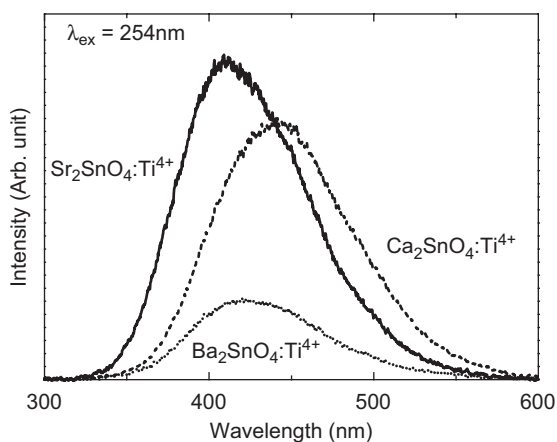


Fig. 3. PL spectra of $\text{Ca}_2(\text{Sn}_{0.95}\text{Ti}_{0.05})\text{O}_4$ (dashed line), $\text{Sr}_2(\text{Sn}_{0.95}\text{Ti}_{0.05})\text{O}_4$ (solid line), and $\text{Ba}_2(\text{Sn}_{0.95}\text{Ti}_{0.05})\text{O}_4$ (dotted line) under UV excitation ($\lambda_{\text{ex}} = 254 \text{ nm}$).

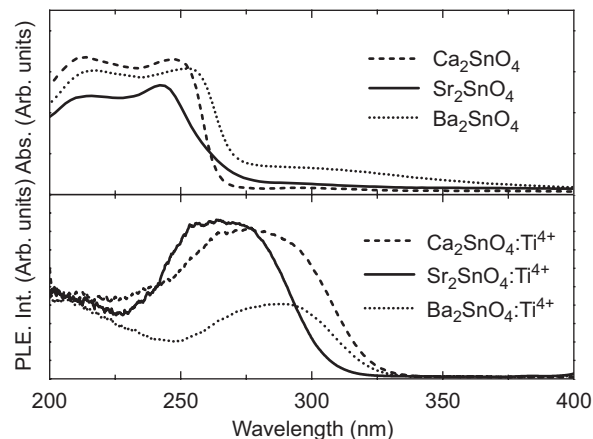


Fig. 4. Excitation spectra of $A_2(\text{Sn}_{1-x}\text{Ti}_x)\text{O}_4$ ($A = \text{Ca}, \text{Sr}, \text{Ba}$) ($x = 0.05$) along with absorption spectra of nondoped host materials: $\text{Ca}_2(\text{Sn}_{0.95}\text{Ti}_{0.05})\text{O}_4$ ($\lambda_{\text{em}} = 445 \text{ nm}$, dashed line), $\text{Sr}_2(\text{Sn}_{0.95}\text{Ti}_{0.05})\text{O}_4$ ($\lambda_{\text{em}} = 410 \text{ nm}$, solid line), and $\text{Ba}_2(\text{Sn}_{0.95}\text{Ti}_{0.05})\text{O}_4$ ($\lambda_{\text{em}} = 425 \text{ nm}$, dotted line).

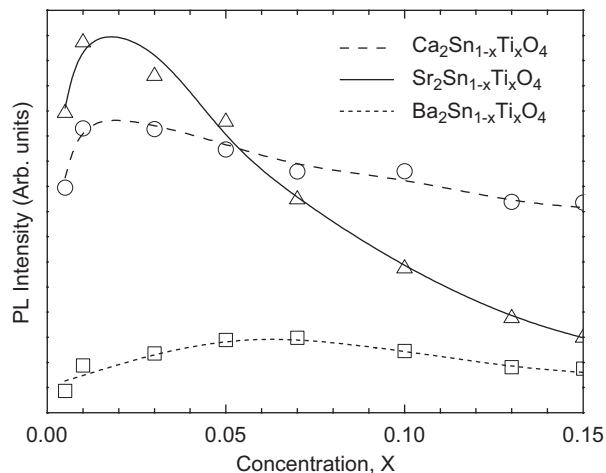


Fig. 5. Relative PL intensities as a function of Ti concentrations, x , in $\text{Ca}_2(\text{Sn}_{1-x}\text{Ti}_x)\text{O}_4$ (dashed line), $\text{Sr}_2(\text{Sn}_{1-x}\text{Ti}_x)\text{O}_4$ (solid line), and $\text{Ba}_2(\text{Sn}_{1-x}\text{Ti}_x)\text{O}_4$ (dotted line).

for the Ca stannate, 1.6 eV for the Sr stannate, and 1.3 eV for the Ba stannate. These large Stokes shifts and the broad emission bands are typical luminescence features of d^0 complex ions [3]. The Stokes shift and PL intensity of the Ba stannate are smaller than the others, probably because the distortion of TiO_6 octahedra in Ba_2SnO_4 is smallest and six Ti–O distances in TiO_6 octahedra are close to each other in Ba_2SnO_4 [13].

Relative emission intensities as a function of Ti concentrations are shown in Fig. 5. The Ti concentration dependence was similar between these samples. In contrast to general rare-earth doped phosphors, the emission intensities in $A_2(\text{Sn}_{1-x}\text{Ti}_x)\text{O}_4$ ($A = \text{Ca}, \text{Sr}, \text{Ba}$) moderately depend on Ti concentrations without showing sharp concentration quenching [8]. Maximum luminescence intensity was observed at $x = 0.01$ – 0.03 for the Ca and Sr stannates and approximately $x = 0.07$ for the Ba

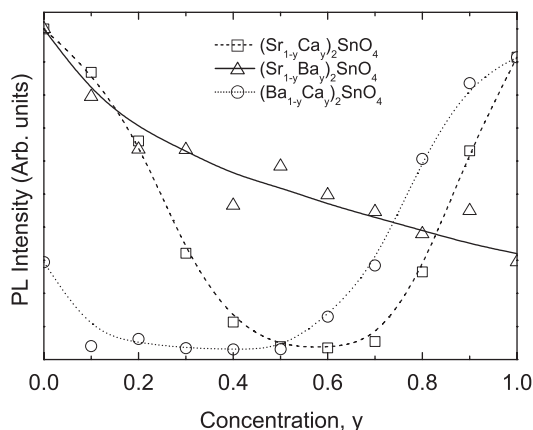


Fig. 6. Relative PL intensities in the $A_2(\text{Sn}_{1-x}\text{Ti}_x)\text{O}_4$ ($A = \text{Ca}, \text{Sr}, \text{Ba}$) ($x = 0.05$) system under UV excitation ($\lambda_{\text{ex}} = 254 \text{ nm}$): $(\text{Sr}_{1-y}\text{Ca}_y)_2\text{SnO}_4:\text{Ti}^{4+}$ (dashed line), $(\text{Sr}_{1-y}\text{Ba}_y)_2\text{SnO}_4:\text{Ti}^{4+}$ (solid line), and $(\text{Ba}_{1-y}\text{Ca}_y)_2\text{SnO}_4:\text{Ti}^{4+}$ (dotted line).

stannate. Ti ions are substituted for Sn ions in distorted SnO_6 octahedra in Ca or Sr stannate, but in almost regular SnO_6 octahedra in Ba stannate. Since the Ti ions themselves also induce the local distortion in the SnO_6 octahedra, the Ti concentration for maximum intensity in the Ba stannate may shift to a higher value than that in the Ca or Sr stannate.

Fig. 6 shows PL intensities in the $A_2(\text{Sn}_{1-x}\text{Ti}_x)\text{O}_4$ ($A = \text{Ca}, \text{Sr}, \text{Ba}$) ($x = 0.05$) system under the UV excitation of $\lambda_{\text{ex}} = 254 \text{ nm}$. The relative intensities are normalized by that of $\text{Sr}_2(\text{Sn}_{0.95}\text{Ti}_{0.05})\text{O}_4$. In the Ti-doped Ca_2SnO_4 – A_2SnO_4 ($A = \text{Sr}$ or Ba) system, each end member once decomposed into $\text{Ca}_{1-z}\text{A}_z\text{SnO}_3$ and $\text{Ca}_{1-z}\text{A}_z\text{O}$ in the intermediate chemical composition without forming a complete solid solution. This is because the crystal structures are different between Ca_2SnO_4 and A_2SnO_4 ($A = \text{Sr}$ or Ba). Simultaneously with the decomposition of the end members, the emission intensities promptly dropped and no enhancement was observed by mixing the alkaline-earth ions. In the Ti-doped Sr_2SnO_4 – Ba_2SnO_4 system, a complete solid solution was formed because of almost the same crystal structures. The emission intensities gradually decreased as Ba concentration increased and no maximum was observed. Therefore, the Ti-doped Sr_2SnO_4 exhibited the strongest blue emission and the formation of solid solution did not increase the PL intensities. These results suggested that local lattice distortions caused by the variation of alkaline-earth ions do not simply increase the luminescence intensity in the Ti-doped A_2SnO_4 ($A = \text{Ca}, \text{Sr}, \text{Ba}$) system, in contrast to the rare-earth doped materials such as $\text{ATiO}_3:\text{Pr}$ and $\text{AHfO}_3:\text{Tm}$ ($A = \text{Ca}, \text{Sr}, \text{Ba}$) [14,15].

Photoluminescence properties of Ti-doped ASnO_3 ($A = \text{Ca}, \text{Sr}, \text{Ba}$) with perovskite structure were also examined. However, blue luminescence was not observed in Ti-doped ASnO_3 . We consider that TiO_6 complexes are possible emission centers and the isolation of the complexes in the crystal structures is important for radiative transition [13]. Ti–O bonds in TiO_6 complexes will include some covalent character and need to compete with neighboring

Sn–O bonds in these stannates to draw O ions to the Ti sides for the formation of the complexes. All six O ions around a Ti ion are next to Sn ions in Ti-doped ASnO_3 , while only four O ions in Ti-doped A_2SnO_4 . This local structural difference seems to make it difficult to form TiO_6 complexes in the three-dimensional ASnO_3 perovskite. Therefore, it is suggested that the blue luminescence is not observed in ASnO_3 but $\text{A}_2(\text{Sn}_{1-x}\text{Ti}_x)\text{O}_4$ ($A = \text{Ca}, \text{Sr}, \text{Ba}$), where SnO_6 octahedra are connected in the low dimensional form and TiO_6 complexes are isolated at low Ti concentration.

4. Conclusion

Ti-doped alkaline-earth stannates, $\text{A}_2(\text{Sn}_{1-x}\text{Ti}_x)\text{O}_4$ ($A = \text{Ca}, \text{Sr}, \text{Ba}$), were prepared by simple solid-state reactions in air and intense blue luminescence was observed under UV excitation at room temperature. In the PL emission/excitation spectra, these Ti-doped stannates exhibited broad emission/excitation bands probably originating from TiO_6 complexes. Mixing of alkaline-earth ions at A sites in this system did not increase the luminescence intensity. By comparison between ASnO_3 and $\text{A}_2(\text{Sn}_{1-x}\text{Ti}_x)\text{O}_4$ ($A = \text{Ca}, \text{Sr}, \text{Ba}$), it was suggested that low dimensional structure of SnO_6 octahedra is important to isolate TiO_6 complexes and activate them as emission centers.

References

- [1] S. Shionoya, W.M. Yen (Eds.), Phosphor Handbook, CRC Press, Boca Raton, FL, 1998.
- [2] W.M. Yen, M.J. Weber, Inorganic Phosphors, CRC Press, Boca Raton, FL, 2004.
- [3] G. Blasse, B.C. Grabmaier, Luminescent Materials, Springer, Berlin, 1994.
- [4] T. Endo, T. Masuda, H. Takizawa, M. Shimada, J. Mater. Sci. Lett. 11 (1992) 1330.
- [5] H. Yamamoto, M. Mikami, Y. Shimomura, Y. Oguri, J. Lumin. 87 (2000) 1079.
- [6] A.J.H. Macke, J. Solid State Chem. 18 (1976) 337.
- [7] E. Danielson, M. Devenny, D.M. Giaquinta, J.H. Golden, R.C. Haushalter, E.W. McFarland, D.M. Poojary, C.M. Reaves, W.H. Weingerg, X.D. Wu, Science 279 (1998) 837.
- [8] K. Ueda, T. Yamashita, K. Nakayashiki, K. Goto, T. Maeda, K. Furui, K. Ozaki, Y. Nakachi, S. Nakamura, M. Fujisawa, T. Miyazaki, Jpn. J. Appl. Phys. 45 (2006) 6981.
- [9] F.A. Kröger, Some Aspects of the Luminescence of Solids, Elsevier, Amsterdam, 1948.
- [10] M. Troemel, Zeitschrift fuer Anorganische und Allgemeine Chemie 371 (1969) 237.
- [11] M.A. Green, K. Prassides, P. Day, J.K. Stalick, J. Chem. Soc. Faraday Trans. 92 (1996) 2155; W.T. Fu, D. Visser, D.J.W. Ijdo, J. Solid State Chem. 169 (2002) 208; W.T. Fu, et al., J. Solid State Chem. 177 (2004) 4081.
- [12] M.A. Green, K. Prassides, P. Day, J.K. Stalick, J. Chem. Soc. Faraday Trans. 92 (1996) 2155; B.J. Kennedy, Aust. J. Chem. 50 (1997) 917.
- [13] B. Bouma, G. Blasse, J. Phys. Chem. Solids 56 (1995) 261.
- [14] T. Kyomen, R. Sakamoto, N. Sakamoto, S. Kunugi, M. Itoh, Chem. Mater. 17 (2005) 3200.
- [15] N. Arai, T.W. Kim, H. Kubota, Y. Yamamoto, H. Koinuma, Appl. Surf. Sci. 197–198 (2002) 402.